Niobium Hot Electron Bolometer Development for a Submillimeter Heterodyne Array Camera

Matthew O. Reese, Daniel F. Santavicca, Luigi Frunzio, and Daniel E. Prober

***Abstract*—We are developing a proof-of-concept for a diffusion cooled hot electron bolometer (HEB) array submillimeter camera. The ultimate objective is to create a working 64 pixel array with the University of Arizona for use on the Heinrich Hertz Telescope. We have fabricated Nb HEBs using a novel angle deposition process. We have characterized these devices using heterodyne mixing at 20 GHz. We also report on optimizations in the fabrication process that improve device performance and a dc screening test for device quality. Using this process, HEBs with a sharp resistive transition (<300 mK) can consistently be produced. These devices have good suppression of superconductivity in the contact pads, with a pad transition ∼1 K below the main bridge transition. Furthermore, the bandwidth was investigated above and below the pad transition and found to be ∼15% larger for 400 nm long bridges with non-superconducting contact pads.**

***Index Terms*—Electron-beam fabrication, hot electron bolometers, superconductivity proximity effect.**

I. Introduction

A superconducting microbridge connected to thick, normal metal contacts forms the active element of the superconducting Hot Electron Bolometer (HEB), which has demonstrated promising performance as a terahertz detector [1]–[5]. HEBs have several desirable characteristics: unlike SIS tunnel junctions, they are not limited by the gap frequency [6]; they require very small local oscillator power; their simple geometry, with low stray impedance, facilitates integration in multi-pixel arrays; and they have demonstrated IF bandwidth as large as 9 GHz [1]–[5].

Recently, we have fabricated diffusion-cooled niobium HEBs. These devices are being developed for a large format array camera for use in the 810 GHz atmospheric window on the Heinrich Hertz Telescope operated by the University of Arizona. This can serve as a model for future THz camera designs. We require a reasonably sharp resistive transition of the superconductor, a critical temperature ($\mathrm{T_c}$) of 4–5 K to operate in a pumped $^4\mathrm{He}$ cryostat, and contact pads that either do not superconduct or have a much lower $\mathrm{T_c}$ than the bridge. Here we present our new fabrication process along with initial characterization results. This process can consistently produce high quality devices, having produced hundreds. Three are discussed.

Manuscript received August 29, 2006. This work was supported in part by NSF-AST, and in part by NASA-JPL. The work of M. O. Reese was supported by a NASA Graduate Student Research Fellowship.

The authors are with the Department of Applied Physics, Yale University, New Haven, CT 06520-8284 USA (e-mail: daniel.prober@ yale.edu).

Color versions of Figs. 2, 3, and 5 are available online at http://ieeexplore.ieee.org.

Digital Object Identifier 10.1109/TASC.2007.898195

II. Fabrication Method

The essential goal has been to produce Nb HEBs using a single lithographic patterning and no cleaning step between the deposition of the Nb and the normal metal of the contact pad. (Here we use Al, because $\mathrm{T_{bath}} > \mathrm{T_{c,Al}}$). Such a process has numerous advantages. First, it is relatively simple. Previously, diffusion-cooled Nb HEBs have been made in complicated multi-step processes requiring as many as five separate metal vacuum deposition steps, two to three photolithography steps and two to three electron beam lithography steps, as well as a reactive ion etching step [7], [8]. Our process requires only one electron beam lithography step and one metal vacuum deposition step. Furthermore, the previous methods required processing steps that could result in degradation of the Nb film after its deposition, whereas ours does not. Last, device to device performance across even a single wafer proved to be variable in the original process for making Nb HEBs. One possibility for this variability was that the argon plasma step used to remove the Au capping layer affected the Nb bridge underneath in an inconsistent fashion, since there was no etch selectivity. The argon plasma etched Nb at a similar rate as Au. By avoiding an etch step, device to device variability may be minimized.

Our structure is patterned as shown in Fig. 1. We use a converted Scanning Electron Microscope (FEI Sirion XL40) to expose a pattern in a 380 nm thick monolayer of 950 K polymethyl methacrylate (PMMA) spun on a substrate of silicon or fused silica. [When using fused silica, we evaporate 10–15 nm of Al on top of our PMMA before e-beam writing, to reduce charging effects. Before developing our resist, we remove the Al with a 5 min. etch in MF-312 developer (4.9% by volume tetra methyl ammonium hydroxide in water), then arrest the process with 20 s in isopropyl alcohol (IPA).] Developing is done in a solution at 25°C of 1:3 methyl isobutyl ketone:IPA for 20 s in an ultrasonic bath, arrested by 20 s in IPA in ultrasound. The substrate is then blown dry with $\mathrm{N_2}$. The sample is loaded into a Kurt J. Lesker Supersystem III Series multi-sputtering and evaporation system with a base pressure of $\sim 10^{-6}$ Pa. First the 2″ diameter Nb target is pre-sputtered for 2 min in an Ar plasma with a power of 350 W and a pressure of 0.17 Pa and a flow rate of ∼82 sccm. The sample is then ion beam cleaned by Ar with current of 4.7 mA for 15 s using a 3 cm Kaufman-type gun to help adhesion to the substrate. Then, a Nb film is sputtered for 9 s, using the same parameters as stated above. And then, with as little delay as possible (typically ∼3 min.), we angle evaporate 200 nm of Al at 1 nm/s [9]. The system has a rotating "J-arm"

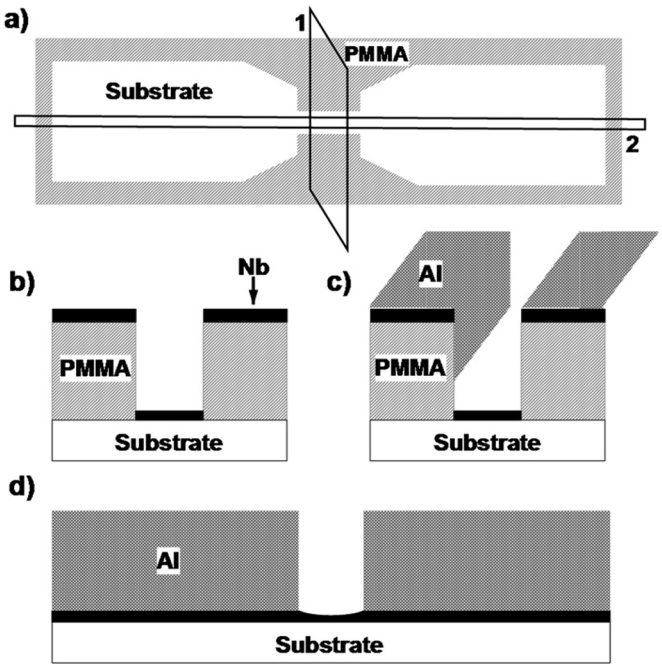

Fig. 1. Deposition process: a) e-beam pattern PMMA, top view [Fig. 1b and 1c are side views of slice 1, Fig. 1d is a side view of slice 2]; b) sputter Nb; c) angle evaporate Al, Al sticks on side of resist in bridge region; d) final result after liftoff. The Nb in the bridge center is slightly thinner than the contact region (see text).

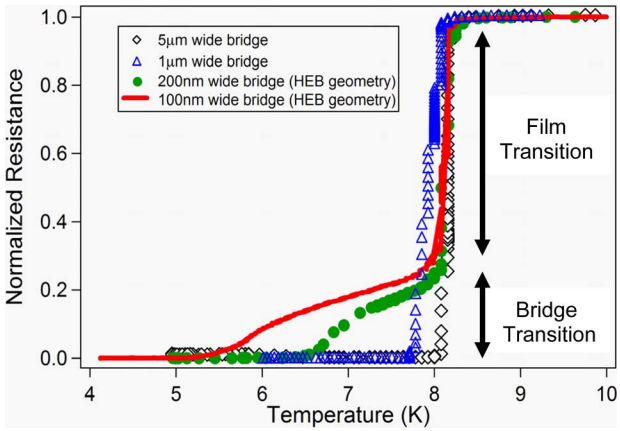

Fig. 2. Transition temperature of 30 nm thick (as measured in the contact pad region) unoptimized Nb films with no Al on top. These films were patterned with the lift-off process described in this paper. The onset of each transition begins at the same point. The sharp transition of each sample is due to the many squares of the contact structure, the widening of these transitions should not be confused with the foot structure in Fig. 4. The increase in ΔT_c for the narrower samples is due to a change in thickness in the bridge structure.

on which the sample is held during the deposition. By rotating the J-arm to different positions in the chamber different sources may be selected. To achieve angle evaporation in this system, the J-arm is rotated to a position so that it is not directly above the evaporation source. Using geometry, the angle may be precisely calculated (the plane of the J-arm is vertically separated from the source by 6.75″). For this work, an angle of 40° was used (with 0° indicating normal incidence). Lift-off is done in hot acetone (50°C) for one hour, followed by 2 min of ultrasonic agitation.

III. Results and Optimizations

A. Monolayer Resist

Initially, we used a bilayer resist process (PMMA on top of the copolymer MMA) designed to allow clean liftoff. This works well with sputtered Nb and even with the directionality of evaporated Al films. However, while liftoff was clean, our sputtered Nb HEBs had broad resistive transitions. This resulted from the relatively non-directional nature of sputtering. The Nb spread out to the base of the bottom resist layer, which was 100–200 nm wider than the opening in the top layer. Hence, the Nb in the center of a 200 nm wide bridge was only ∼60% of the thickness of the contact pads, from spreading of the Nb after it had passed through the narrow opening in the top resist layer. The T_c dependence on film thickness, thus led to broad resistive transitions in these devices.

Using a single layer of resist significantly reduced the effect of Nb spreading. As the bridge becomes increasingly narrow ($< 1\ \mu m$), however, a reduction of the bridge thickness is still observed. This can be seen in Fig. 2 by the broadening of the resistive transitions for narrow bridges. This effect is due to the sputter process and the geometry of the PMMA slot used to form the HEB. In sputtering, atoms arrive at the substrate from a wide range of angles. For a large opening in the resist pattern, sputtered material from every direction reaches the substrate. In a narrow opening, only a fraction of the incident Nb reaches the substrate (some hits the resist and sticks to it, while the remainder scatters down to the bridge), thereby reducing the deposited thickness in the center of the wire (bridge) compared to the contact pad region. This reduced thickness leads to a broader transition at a lower temperature for the bridge compared to the contact pads.

Liftoff can be more difficult with a monolayer resist, but the region of the most concern is around the bridge. Since the bridge is very thin (∼10 nm), and the resist is thick (∼380 nm), liftoff in this region is not a problem. While some flagging (poor liftoff) results in the contacts due to the thick (200 nm) Al that is angle evaporated into the resist sidewall [Fig. 1], this effect is minimal and is far removed from the bridge. On all other edges of the structure there is little to no flagging of the Al film because the resist is almost twice as thick as the Al.

B. Improved Nb

The large ΔT_c for the bare Nb films for a HEB geometry (i.e., a narrow wire bridge 400 nm long) made with our liftoff process is shown in Fig. 2. This highlights the difficulty the thickness variation can pose in obtaining a sharp resistive transition (small ΔT_c), which is a critical feature for a hot electron bolometer. Here, the sharp transition is from the contact pad region, which has a large number of squares. The resistive transition spreads out with the narrowing of the patterned bridge. The large ΔT_c stems from the large dependence of the critical temperature our unoptimized Nb films had on thickness [see Fig. 3]. We were able to improve the quality of our thin film Nb, as determined by its T_c, by lowering our Ar plasma pressure and at the same time increasing the dc power [see Fig. 3]. Our original values for

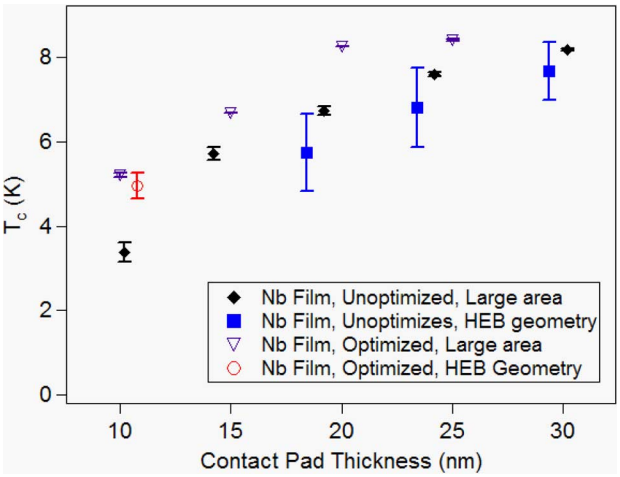

Fig. 3. Transition temperature of Nb Films with no Al on top. The error bars represent the onset and completion of the transition (T_c is defined as the center of the transition). The points are spread out horizontally to allow easier viewing, and suggest the error in thickness measurements. The thicknesses are 10, 14, 19, 24, and 30 nm, measured in the contact pad region.

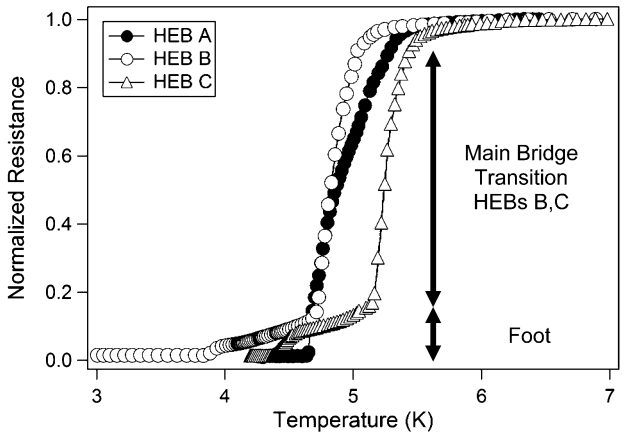

Fig. 4. Normalized resistance versus temperature curves for three HEBs. See Table for details on fabrication parameters. Notice the foot structure for devices B and C due to the contact pads. The broad resistive transition of Device A may be a result of poor suppression in the contact pads as well.

Ar pressure and power were 0.53 Pa/270 W; our new values are 0.17 Pa/350 W. This increased our deposition rate from 1.0 nm/s to 1.25 nm/s and may have reduced the film stress (as well as incorporation of oxygen) and thus improved the film quality [10]. By improving the quality of the Nb, we reduced the dependence of T_c on thickness [Fig. 3]. When the experiment from Fig. 2 was repeated for optimized Nb (not shown), ΔT_c was reduced to 300 mK or less (depending on bridge width). This makes possible HEBs with sharp bridge transitions as shown in Fig. 4. The optimized Nb used to make these HEBs was about one third the thickness of that used in the bare films in Fig. 2.

C. Suppression of Superconductivity in the Contact Pads

In a diffusion-cooled hot electron bolometer, we want to form a clean interface in the contact pads, thereby ensuring good suppression of the superconductivity in the thin Nb under the thick Al. The presence of a superconducting energy gap in the pads would inhibit the ability of hot electrons to diffuse off the bridge.

TABLE I
FABRICATION PARAMETERS FOR THE HOT ELECTRON BOLOMETERS APPEARING IN FIG. 4

	Estimated Nb Thickness	Base Pressure	Δt: Nb→Al
HEB A	10 nm	4 x 10^{-5} Pa	35 min
HEB B	10 nm	4 x 10^{-5} Pa	6 min
HEB C	12 nm	1 x 10^{-5} Pa	37 s

The proximity effect has a strong dependence on both the thickness of the Nb and Al films as well as the transparency of the interface between them. Hence, it can be difficult to achieve good suppression [11], [12]. We found that the thicknesses of our Nb and Al films, as well as the length of time between their depositions, significantly affect suppression.

We first achieved good suppression in the contact pads (while still having an acceptably high T_c in the bridge) by reducing the time delay between depositions. Our improved Nb films have increased T_c and reduced ΔT_c. This allows for thin (∼10 nm) Nb films, which are more readily suppressed. We also use a thick (200 nm) normal metal film. By reducing the base pressure of our system from 4×10^{-5} to 1×10^{-6} Pa, we were able to make the time interval between depositions relatively unimportant. With $P = 10^{-6}$ Pa we could get the same suppression if we waited 30 s or 30 min. With our higher quality Nb film parameters and 200 nm Al, at a base pressure of 4×10^{-5} Pa, we made two batches of devices with a long (HEB A) and shorter (HEB B) time interval between the Nb and Al depositions to illustrate the importance of interface transparency [Table I, Fig. 4].

HEB A has a single, somewhat spread out transition. The contact pads have a higher onset transition temperature than the bridge, because the Nb film in the contacts pads is thicker than in the bridge, and was only weakly suppressed. HEBs B and C each had short intervals between depositions and each has two distinct transitions. The higher temperature transition is the bridge transition; the second is due to the transition of the suppressed contact pads. The transition temperature of the contact pads (∼3.8 K for HEB B, ∼4.4 K for HEB C which had thicker Nb) agrees with that of Nb-Al bilayers made during the same deposition but measured separately. The finite resistance remaining at temperature below the bridge transition is largely a result of the ends of the bridge being proximitized normal by the normal contact pads (for HEB B this occurs between 4.0 K and 4.7 K-below 4 K the contacts are superconducting) [13], [14]. This "foot" structure thus provides a clear indication the interface between the Al and Nb in the contacts is clean and transparent. Furthermore, if this structure is not present, as for HEB A, the pads transition at or above the T_c of the bridge. If this is the case, then the outdiffusion of hot electrons off the bridge will be restricted, degrading device performance.

D. Improved Bandwidth

To illustrate the importance of good suppression of the superconductivity of the contact pads, we provide bandwidth measurements in the overpumped regime, where the critical current is suppressed by the local oscillator power. These were performed at temperatures above and below the T_c of the contact pads. These data are from HEB C, a 400 nm long device,

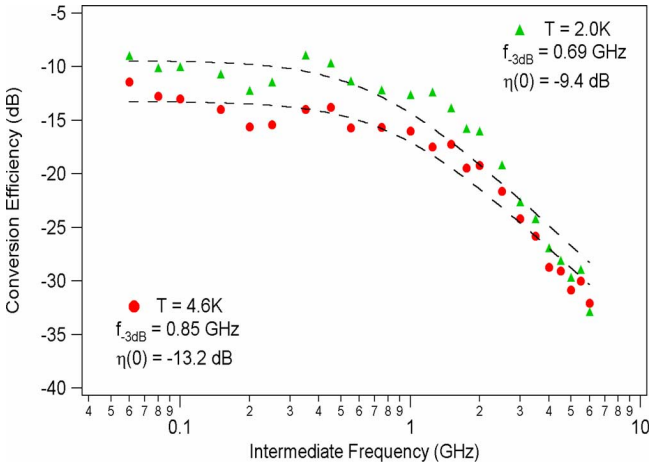

Fig. 5. IF conversion efficiency of HEB C with bandwidth above and below the transition of the suppressed contact pads. The contact pads in this sample had a $T_c = 4.4$ K.

from the same cooldown [Fig. 5]. These results were obtained by heterodyne mixing at 20 GHz following the techniques described in [15] and [16], [17]. We used wirebonds, however, instead of a flip-chip process to connect the device. The larger conversion efficiency (for $T = 2.0$ K) can be explained by the increase of conversion efficiency as the bath temperature is lowered to $T_{bath} \approx T_c/2$ [15]. There is an observed increase of $\sim$15% of the IF bandwidth when the contact pads are normal, at $T = 4.6$ K. The reduced bandwidth at $T = 2.0$ K is partly due to hot electrons at energies less than the gap of the contact pads that cannot easily diffuse off the nearly normal bridge. This increases the thermal response time and thus reduces the IF bandwidth. At 4.6 K, the gap in the contacts is zero and all the hot electrons are able to leave the bridge rapidly. A larger effect, however, is likely the effective reduction in bridge length from the proximitized normal ends of the bridge. The bandwidth, to the authors' knowledge, has not previously been observed to exhibit any temperature dependence in a diffusion-cooled device. While this effect is intriguing and large bandwidths are desirable, a two GHz IF bandwidth can readily be achieved by reducing the bridge length to 250 nm [16], [17].

IV. Summary and Future Plans

A novel, robust, high-yield fabrication process to produce high quality superconducting hot electron bolometers was developed and described in detail. The simplicity of process marks a major improvement over previous work. Furthermore, the necessary optimizations to make high quality HEBs were described together with a straightforward dc screening test, measurement of R(T) to observe a foot structure as in Fig. 3. The bandwidth of the devices was also investigated above and below the pad transition and found to vary by $\sim$15% for 400 nm long bridges.

In the future, we seek to reduce further the T_c of the contact pads, thereby allowing us to operate at 2 K and maximize both conversion efficiency and bandwidth. We also plan to investigate the mixer noise and conversion efficiency at 345 and 810 GHz in measurements at the University of Arizona.

Acknowledgment

We thank B. Reulet, L. Spietz, and J. D. Teufel for helpful discussions.

References

[1] E. M. Gershenzon, G. N. Gol'tsman, I. G. Gogidze, Y. P. Gusev, A. I. Elant'ev, B. S. Karasik, and A. D. Semenov, "Millimeter and submillimeter range mixer based on electronic heating of superconducting films in the resistive state," *Sov. Phys. Supercond.*, vol. 3, no. 10, pp. 1582–1597, 1990.

[2] D. E. Prober, "Superconducting terahertz mixer using a transition-edge microbolometer," *Appl. Phys. Lett.*, vol. 62, pp. 2119–2121, 1993.

[3] J. J. A. Baselmans, M. Hajenius, J. R. Gao, T. M. Klapwijk, P. A. J. de Korte, B. Voronov, and G. Gol'tsman, "Doubling of sensitivity and bandwidth in phonon cooled hot electron bolometer mixers," *Appl. Phys. Lett.*, vol. 84, pp. 1958–1960, 2004.

[4] R. A. Wyss, B. S. Karasik, W. R. McGrath, B. Bumble, and H. G. LeDuc, "Noise and bandwidth measurements of diffusion-cooled Nb hot electron bolometer mixers at frequencies above the superconductive energy gap," in *Proc. 10th Int. Symp. Space Terahertz Tech.*, 1999, pp. 215–217.

[5] B. S. Karasik, M. C. Gaidis, W. R. McGrath, B. Bumble, and H. G. LeDuc, "A low noise 2.5 THz superconductive Nb hot-electron mixer," *IEEE Trans. Appl. Supercond.*, vol. 7, pp. 3580–3583, 1997.

[6] M. Bin, M. C. Gaidis, J. Zmuidzinas, and T. G. Phillips, "Quasi-optical SIS mixers with normal metal tuning structures," *IEEE Trans. Appl. Supercond.*, vol. 7, pp. 3584–3588, 1997.

[7] B. Bumble and H. G. LeDuc, "Fabrication of a diffusion cooled superconducting hot electron bolometer for THz mixing applications," *IEEE Trans. Appl. Supercond.*, vol. 7, pp. 3560–3563, 1997.

[8] K. Fiegle, D. Diehl, and K. Jacobs, "Diffusion-cooled superconducting hot electron bolometer heterodyne mixer between 630 and 820 GHz," *IEEE Trans. Appl. Supercond.*, vol. 7, pp. 3552–3555, 1997.

[9] G. J. Dolan, "Offset masks for lift-off photoprocessing," *Appl. Phys. Lett.*, vol. 31, pp. 337–339, 1977.

[10] S. Knappe, C. Elster, and H. Koch, "Optimization of niobium thin films by experimental design," *J. Vac. Sci. Technol. A*, vol. 15, pp. 2158–2166, 1997.

[11] J. M. Martinis, G. C. Hilton, K. D. Irwin, and D. A. Wollman, "Calculation of T_c in a normal-superconductor bilayer using the microscopic-based Usadel theory," *Nucl. Instrum. Methods A*, vol. 444, pp. 23–27, 2000.

[12] D. Esteve, H. Pothier, S. Gueron, N. O. Birge, and M. Devoret, *Correlated Fermions and Transport in Mesoscopic Systems*, T. Martin, G. Montambaux, and J. T. T. Ran, Eds. : , 1996.

[13] D. W. Floet, J. J. A. Baselmans, T. M. Klapwijk, and J. R. Gao, "Resistive transition of niobium superconducting hot-electron bolometer mixers," *Appl. Phys. Lett.*, vol. 73, pp. 2826–2828, 1998.

[14] I. Siddiqi, A. Verevkin, D. E. Prober, A. Skalare, W. R. McGrath, P. M. Echternach, and H. G. LeDuc, "Heterodyne mixing in diffusion-cooled superconducting aluminum hot-electron bolometers," *J. Appl. Phys.*, vol. 91, pp. 4646–4654, 2002.

[15] P. J. Burke, "High frequency electron dynamics in thin film superconductors and applications to fast, sensitive THz detectors" Ph.D. dissertation, Yale Univ., New Haven, CT, 1998 [Online]. Available: http://www.yale.edu/proberlab/alumni.html

[16] P. J. Burke, R. J. Schoelkopf, D. E. Prober, A. Skalare, W. R. McGrath, B. Bumble, and H. G. LeDuc, "Length scaling of bandwidth and noise in hot-electron superconducting mixers," *Appl. Phys. Lett.*, vol. 68, pp. 3344–3346, 1996.

[17] P. J. Burke, R. J. Schoelkopf, D. E. Prober, A. Skalare, B. S. Karasik, M. C. Gaidis, W. R. McGrath, B. Bumble, and H. G. LeDuc, "Mixing and noise in diffusion and phonon cooled superconducting hot-electron bolometers," *J. Appl. Phys.*, vol. 85, pp. 1644–1653, 1999.